shown that As vacancies on the GaAs(110) surface preferentially move between zigzag chains (*12*). This phenomenon can be understood in terms of simple bond-breaking and rebinding arguments (*12*). The observed migration of vacancies can be explained by the same arguments.

The motion of the defects could be thermally induced or the result of mechanical transfer of the atoms by the tip. In some cases, during the continuous observation of the same area, defects appeared and disappeared. The position changes were independent of the scanning direction, which indicates a thermal origin for the defect motion, but the present data is not sufficient to exclude other mechanisms. Quantitative comparison with STM imaging is necessary.

REFERENCES AND NOTES

1. D. M. Eigler and E. K. Schweizer, *Nature* **344**, 524 (1990); L. J. Whitman, J. A. Stroscio, R. A. Dragoset, R. J. Celotta, *Science* **251**, 1206 (1991); I.-W. Lyo and Ph. Avouris, *ibid.* **253**, 173 (1991).
2. Ph. Ebert, G. Cox, U. Poppe, K. Urban, *Ultramicroscopy* **42–44**, 871 (1992).
3. Ph. Ebert, M. G. Lagally, K. Urban, *Phys. Rev. Lett.* **70**, 1437 (1993).
4. G. Binnig, C. F. Quate, Ch. Gerber, *ibid.* **56**, 930 (1986).
5. F. J. Giessibl, *Science* **267**, 68 (1995); S. Kitamura and M. Iwatsuki, *Jpn. J. Appl. Phys.* **34**, L145 (1995).
6. M. Ohta *et al.*, *J. Vac. Sci. Technol. B* **12**, 1705 (1994).
7. D. Rugar, H. J. Mamin, P. Guethner, *Appl. Phys. Lett.* **55**, 2588 (1989).
8. T. R. Albrecht, P. Grütter, D. Horne, D. Rugar, *J. Appl. Phys.* **69**, 668 (1991).
9. R. J. Meyer *et al.*, *Phys. Rev. B* **22**, 6171 (1980).
10. M. Ohta *et al.*, *J. Vac. Sci. Technol. B* **13**, 1265 (1995).
11. Ph. Ebert, K. Urban, M. G. Lagally, *Phys. Rev. Lett.* **72**, 840 (1994).
12. G. Lengel, M. Weimer, J. Gryko, R. E. Allen, *J. Vac. Sci. Technol. A* **12**, 1855 (1994).
13. We thank F. Osaka and S. Ohkouchi of Optoelectronics Technology Research Laboratory and M. Suzuki of Nippon Telegram and Telephone Interdisciplinary Research Laboratories for valuable discussions. We thank S. Mishima of Olympus Optical for technical support. M.O. is a Research Fellow of the Japan Society for the Promotion of Science. Part of this work was supported by a Grant-in-Aid for Scientific Research from the Ministry of Education, Science, and Culture.

27 July 1995; accepted 11 October 1995

Behavior of the Heliosphere over Prolonged Solar Quiet Periods by ^{44}Ti Measurements in Meteorites

G. Bonino,* G. Cini Castagnoli, N. Bhandari, C. Taricco

The heliospheric magnetic field (HMF) is controlled by solar activity, as established by measurements over the last few decades, but its characteristics when the sun was quiet for prolonged periods, such as during Gleissberg or Maunder minima, are not known. Titanium-44, produced in meteorites, provides a monitor of the galactic cosmic ray (GCR) flux and allows estimation of the modulation effect of the sun for the period 1883 to 1992. The titanium-44 activity is consistent with the expected value, but the increase, due to the last Gleissberg minimum, is four times greater than expected for a GCR modulation based solely on sunspot numbers. This result implies that the HMF was weaker than at present and as a result the GCR flux (for energy greater than 1 gigaelectron volt) was higher between 2.2 to 3.6 protons per square centimeter per second per 4π steradians at 1 to 3 astronomical units in solar cycles 12 to 15.

Production of cosmogenic radioisotopes in meteorites depends on the GCR flux, which is controlled by the HMF which, in turn, depends on solar activity. GCR flux is inversely correlated with sunspot number. The radioisotopes can, therefore, serve as proxy records of solar activity. This approach has been used to understand solar behavior in the past based on records from terrestrial archives, such as ^{14}C in tree rings (*1*) and ^{10}Be in ice cores (*2*) and sediments, but such records are not free from interference of the terrestrial climate that governs the deposition rates of these isotopes in various terrestrial reservoirs (*1*). A similar approach, that of using isotopes produced in meteorites, offers a direct assessment of the solar activity, free from the influence of climatic cycles on Earth. The effect of the 11-year solar cycle has been quantitatively estimated by analysis of ^{22}Na (half-life, 2.6 years) in meteorites (*3, 4*) and lunar samples (*5*). Here we use measurements of ^{44}Ti in stone meteorites with known dates of fall to assess century-scale variations in GCR flux.

^{44}Ti has a mean life of about 96 years (*6*) and is thus ideal for monitoring the behavior of the sun during the past 100 or 200 years. It is produced in cosmic-ray interactions (>70 MeV) in meteoritic iron and nickel (*7*). Attempts to determine its variation by radiochemical separation in several meteorites have not yielded measurable activity (*8*) because its production cross section is low, resulting in ^{44}Ti activity of about 1 dpm per kilogram of chondrite. We have therefore designed (*9*) a sensitive and selective γ-ray spectrometer to measure activity of its daughter, ^{44}Sc (half-life, 3.93 hours), which is in secular equilibrium with its parent, ^{44}Ti. ^{44}Sc decays by β^+ emission in coincidence with a 1157-keV γ-ray. Interference from the ubiquitous, naturally occurring ^{214}Bi (1155 keV) can be suppressed when the Ge detector is used in coincidence with a surrounding NaI(T) detector that operates only in annihilation γ-ray windows. By situating the spectrometer at an equivalent water depth of 70 m under Monte dei Cappuccini in Torino in a nitrogen atmosphere, a background of ~0.6 counts per day in 1157-keV channels was achieved.

We counted 10 fragments of nine chondrites: Alfianello (L6, 625 g), Lancon (H6, 1080 g), Holbrook (L6, 331 g), Olivenza (LL5, 247 g), Rio Negro (L4, 388 g), Monze (L6, 165 g), Dhajala (H3, 700 g), Torino (H6, 445 g), and Mbale (L5/6, 700 and 730 g) that fell during the period 1883 to 1992. The activity of ^{26}Al (1809 keV), ^{40}K (1461 keV), and ^{44}Ti (^{44}Sc, 1157 keV) was measured by counting fragments for a period

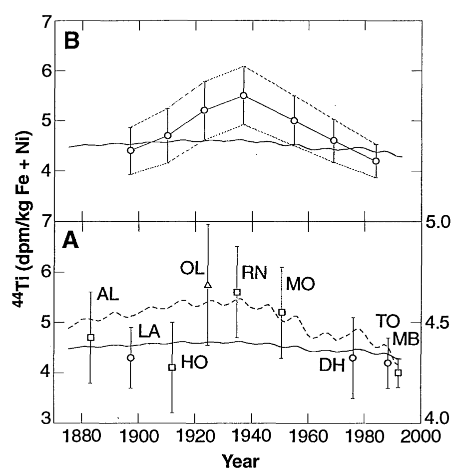

Fig. 1. (**A**) Observed ^{44}Ti activity (dpm per kilogram of Fe + Ni) for H (○), L (□), and LL (△) chondrites. AL, Alfianello; LA, Lancon; HO, Holbrook; OL, Olivenza; RN, Rio Negro; MO, Monze; DH, Dhajala T273; TO, Torino; MB, Mbale-T and Mbale-A. The variation expected due to modulation of GCR by sunspot activity is shown by a thick curve and, on a magnified (right hand) scale, by a dashed curve to illustrate small variations expected due to the Schwabe cycles. (**B**) Comparison of the three-point running mean and the error on the trend (dotted curve) with the expected profile based on the sunspot numbers.

G. Bonino, G. Cini Castagnoli, C. Taricco, Istituto di Cosmogeofisica, Corso Fiumè 4, 10133 Torino, Italy, and Istituto di Fisica Generale dell'Universita', Via Giuria 1, 10125 Torino, Italy.
N. Bhandari, Physical Research Laboratory, Ahmedabad 380009, India.

ranging between 4 to 12 weeks. The inherent ^{40}K concentration in the meteorites was used as an internal standard for determining the effective efficiency of counting for each meteorite fragment, as described (*10*). The measured activity of ^{44}Ti was corrected for decay to the time of fall (Table 1 and Fig. 1A).

To determine the cosmic ray flux responsible for production of the observed activity of ^{44}Ti, it is necessary to correct for (i) variation in target element (Fe and Ni) concentration and (ii) shielding depth within the meteorite. The shielding correction was made on the basis of the density of tracks produced by cosmic ray heavy nuclei (*11*), which were measured in several spot samples of each meteorite. Together with exposure ages, calculated from cosmogenic ^{21}Ne (*12*), the track density allowed us to determine the preatmospheric size (R_o) and shielding depths (Δx) of the meteorite fragments (*11*). Further constraints on the shielding depths were obtained by comparison of ^{26}Al activity with the production depth profiles (*13*). Measurements of ^{44}Ti in two fragments of Mbale ($\Delta x = 12$ and $\sim$40 cm) indicated that the change in ^{44}Ti production rate with depth was small, as expected for high-energy products. The shielding depths of all the meteorite fragments were estimated to lie between a narrow range of 8 to 25 cm and, except for Olivenza and Dhajala, R_o of all meteorites was between 23 and 40 cm. Olivenza and Dhajala were larger bodies in space (estimated R_o, 85 and 110 cm, respectively). The shielding correction, normalized to Torino ($[R_o, \Delta x] = [24, 16]$ cm), was small in all meteorites except Dhajala and the Mbale (T) fragment, where it approached 10%.

The observed ^{44}Ti activity was compared with the expected value calculated from the isotope production model (*14*) (Fig. 1A). The model requires inputs of GCR flux, J_G (protons >1 GeV/cm^2·s·4π sr), and excitation functions of ^{44}Ti from Fe and Ni. $J_G(t)$, appropriately modulated by the solar activity, was calculated on the basis of sunspot numbers (Fig. 2A) and Climax neutron monitor count rates (N_m) as follows.

The relation between $N_m(t)$ and annual sunspot numbers, $R(t)$, for the period 1953 to 1992 is given by

$$N_m(t) = 4265.133 - 3.961559[R(t-1)] - 0.0116098[R(t-1)]^2 + 6.018108 \times 10^{-5}[R(t-1)]^3$$

This relation was extrapolated back to 1800. J_G was then calculated by a linear regression between the normalized (January 1965: 4291.7 counts/hour × 100 = 1) neutron monitor rate, $N_m{}^*$, as given by

$$J_G = 8.13N_m{}^* - 5.845$$

as described (*10*). The flux, used with the isotope production model (*14*), gives the expected profile of ^{44}Ti as a function of time of fall (Figs. 1 and 2B). A systematic error may be present in the absolute production rate as a result of uncertainties inherent in the model and the excitation function, but the shape of its time profile depends only on the variation in sunspot numbers (Fig. 2A). The small oscillations in production rates (Fig. 2B) are due to the 11-year Schwabe cycle and the two large maxima are due to the Gleissberg minima, with a phase lag due to the integrating nature of the ^{44}Ti activity over its mean life.

The agreement between the observed ^{44}Ti activity and the expected values (Fig. 1A) is reasonably good, taking into account the errors of measurement (7 to 20%), and validates the procedure used, except that the activity in meteorites that fell during 1920 to 1950 appears to be higher. To ascertain whether the increase is real or a statistical fluctuation, and to reduce the standard deviations, we consider moving averages of the data. The three-point running mean together with the error band (Fig. 1B) shows a maximum around 1935, indicating that the trend of increased activity is significant. In order to highlight the variability of the data and the phase of the maximum, we show the production profile on a magnified (×4) scale (Fig. 1A, dashed curve). The phase of the observed maximum clearly agrees with that expected due

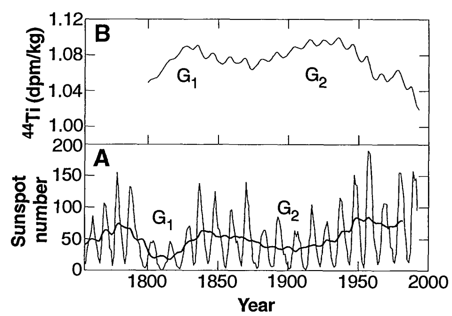

Fig. 2. (**A**) Annual mean sunspot numbers from cycle 1 to 22. The locations of Gleissberg minima of 1810 and 1910 are indicated by G_1 and G_2, respectively. The thick curve shows the 22-year running mean of the sunspot numbers. (**B**) The calculated production rate of ^{44}Ti activity as a function of time based on sunspot numbers given in (A). Curve shows the variation expected due to the 11-year Schwabe cycle and the 90-year Gleissberg cycle. The periods of peak activity expected due to Gleissberg minima G_1 and G_2 are indicated.

Table 1. Track density, calculated shielding depths, and ^{44}Ti activity at the time of meteorite fall. Time of fall is given as date.month.year. Ma, million years ago.

Meteorite (class)	Date of fall	Exposure age (Ma)	Track density (10^5/cm^2)*	Shielding (cm)*	Fe + Ni (%)	^{44}Ti† a	^{44}Ti† b
Alfianello (L6)	16.2.1883	25.3	1.52 (O, 25)	11.5 ± 1	22.95	1.1 ± 0.2	4.7 ± 0.9
Lancon (H6)	20.6.1897	6.6	1.37 (O, 74)	11 ± 3	28.52	1.3 ± 0.2	4.3 ± 0.6
			4.56 (O, 107)	12.5 ± 2.5			
Holbrook (L6)	19.7.1912	16	0.5 (P, 51)	17 ± 2.5	21.6	0.8 ± 0.2	3.8 ± 0.9
			0.8 (P, 15)	12.5 ± 1.5			
			5.0 (P, NR)	9.5 ± 1.5			
Olivenza (LL5)	19.6.1924	11.6	<1	14.5 ± 2.5	20.26	1.2 ± 0.2	5.8 ± 1.2
Rio Negro (L4)	21.9.1934	21.5	0.42 to 5.4 (O, 10 to 78)‡	14 ± 6	22.57	1.3 ± 0.2	5.6 ± 0.9
			1 to 2.59 (P, 22 to 38)‡				
Monze (L6)	5.10.1950	9.9	0.69 (O, 9)	11.6 ± 0.8	22.0	1.1 ± 0.2	5.2 ± 0.9
			0.93 (P, NR)	14.5 ± 2.5			
Dhajala (H3)	28.1.1976	8.9	0.0096§	24	28.74	1.2 ± 0.3	4.4 ± 0.8
Torino (H6)‖	18.5.1988	68	4.2	16 ± 2	27.26	1.2 ± 0.2	4.2 ± 0.5
Mbale-A (L5/6)	14.8.1992	26.9	2.14 to 3.6 (O, 199)	11.6 ± 0.8	22.9	1.0 ± 0.1	4.0 ± 0.4
Mbale-T			<0.2	~40		0.8 ± 0.1	4.0 ± 0.4

*O, Olivines; P, Pyroxenes; number of tracks counted are given in parentheses [NR, not recorded (*11*)]. Mean shielding depth ± range for different fragments was calculated from (*11*). †^{44}Ti activity (a) dpm per kilogram of meteorite, uncorrected for target abundance and shielding; and (b), dpm per kilogram of (Fe + Ni), corrected for shielding and normalized to Torino. ‡Rio Negro has solar flare tracks (*9*), which are not included here. §Data are from (*16*). ‖Track data are from (*10*). Torino had a complex exposure: a long exposure (stage I) and a short exposure (≲10 Ma, stage II). Composite exposure age of 68 Ma was recalculated from (*10*).

to the Gleissberg minimum early in this century. However, the observed increase of about 20% is four times that expected based on the sunspot numbers.

The observed high ^{44}Ti and the inferred high GCR flux during the Gleissberg minimum suggest a much-weakened modulation of GCR during prolonged solar quiet periods. The heliosphere, during the 11-year solar cycles, is divided into two hemispheres of opposite polarity by a wavy heliospheric neutral sheet (HNS) whose inclination to the sun's rotational equator increases from a few degrees at solar minimum to >70° at solar maximum and whose undulations also increase with solar activity (*15*). The HMF is relatively smooth during the solar minima. The enhanced GCR fluxes required for the higher production of ^{44}Ti can be achieved if (i) the HNS becomes smooth and remains close to the helioequator; (ii) the HMF becomes weak, more regular, and orderly; or (iii) the size of the heliosphere shrinks during a prolonged period of low sunspot numbers, so that a larger flux of cosmic rays can enter into the inner heliosphere. The GCR flux, J_G(>1 GeV), near 1 AU during maximum and minimum of the 11-year solar cycle (*14, 16*) in the past four Schwabe cycles, varied between 1.4 and 2.2 to 2.5 protons/$cm^2 \cdot s \cdot 4\pi$ sr, with an average value of 1.7 protons/$cm^2 \cdot s \cdot 4\pi$ sr. The observed activity can be explained if J_G varied between 2.2 and 3.6 protons/$cm^2 \cdot s \cdot 4\pi$ sr at 1 to 3 AU during solar cycles 12 to 15 covering the Gleissberg minimum at the turn of the century. Such a regularity of HMF may also justify the even higher GCR fluxes estimated for the Maunder minimum, when sunspot numbers were low for about 70 years (1645 to 1715), and can explain the high activities of ^{14}C and ^{10}Be observed on Earth (*17*).

REFERENCES AND NOTES

1. M. Stuiver and P. D. Quay, *Science* **207**, 11 (1980); G. Cini Castagnoli and D. Lal, *Radiocarbon* **22**, 133 (1980); P. E. Damon and C. P. Sonett, in *The Sun in Time*, C. P. Sonett, M. S. Giampapa, M. S. Matthews, Eds. (Univ. of Arizona Press, Tucson, 1991), pp. 360–388.
2. J. Beer *et al.*, *Nature* **347**, 164 (1990).
3. J. C. Evans, J. H. Reeves, L. A. Rancitelli, D. D. Bogard, *J. Geophys. Res.* **87**, 5571 (1982).
4. N. Bhandari, G. Bonino, G. Cini Castagnoli, C. Taricco, *Meteoritics* **29**, 443 (1994).
5. R. C. Rancitelli, J. S. Fruchter, W. S. Felix, R. W. Perkins, N. A. Wogman, *Proceedings of the Sixth Lunar Science Conference*, Houston, TX, 17 to 21 March 1975 (Pergamon, New York, 1975), p. 1891; R. C. Reedy, *Proceedings of the Eighth Lunar Science Conference*, Houston, TX, 14 to 18 March 1977 (Pergamon, New York, 1977), p. 825; M. B. Potdar and N. Bhandari, *Proc. Indian Natl. Sci. Acad.* **A45**, 32 (1979).
6. D. E. Alburger and G. Harbottle, *Phys. Rev.* **C41**, 2320 (1990).
7. M. Honda and J. R. Arnold, *Science* **143**, 203 (1960); J. R. Arnold, M. Honda, D. Lal, *J. Geophys. Res.* **66**, 3519 (1960).
8. P. J. Cressy, thesis, Carnegie Institution of Technology, Pittsburgh, PA (1964).
9. G. Bonino, N. Bhandari, G. Cini Castagnoli, *Nuovo Cimento* **15**, 99 (1992); N. Bhandari, G. Bonino, G. Cini Castagnoli, K. M. Suthar, *Proceedings of the 24th International Cosmic Ray Conference*, Rome, Italy, 28 August to 8 September 1995, **SH**9.1, 1181 (1995).
10. N. Bhandari *et al.*, *Meteoritics* **24**, 29 (1989).
11. N. Bhandari *et al.*, *Nuclear Tracks* **4**, 213 (1980).
12. L. Schultz and H. Kruse, *Meteoritics* **24**, 155 (1989).
13. N. Bhandari *et al.*, *Geochim. Cosmochim. Acta* **57**, 2361 (1993).
14. N. Bhandari, *Proc. Indian Acad. Sci.* **90**, 359 (1981).
15. M. S. Potgieter, *Proceedings of the 23rd International Cosmic Ray Conference*, Calgary, Canada, 19 to 30 July 1993, D. A. Leahy, R. B. Hicks, D. Venkatesan, Eds. (World Scientific, Singapore, 1993), pp. 213–242.
16. M. B. Potdar, N. Bhandari, K. M. Suthar, *Proc. Ind. Acad. Sci.* **95**, 169 (1986).
17. M. Stuiver, in *The Solar Engine and Its Influence on Terrestrial Atmosphere and Climate*, E. Nesme-Ribes, Ed., vol. 25 of *Global Environmental Change*, NATO ASI Series, (Springer-Verlag, Berlin, 1994), pp. 203–220; J. Beer, in *ibid.*, pp. 221–233.

18. We are grateful to C. Castagnoli for support and encouragement, to G. V. Coyne and J. Betlem for providing meteorite samples, and to A. Romero and K. M. Suthar for technical assistance.

17 July 1995; accepted 3 October 1995

Particle Formation in the Upper Tropical Troposphere: A Source of Nuclei for the Stratospheric Aerosol

C. A. Brock,* P. Hamill, J. C. Wilson, H. H. Jonsson, K. R. Chan

Atmospheric measurements and numerical calculations described here indicate that binary homogeneous nucleation of H_2SO_4-H_2O particles occurs in the upper tropical troposphere. Particle concentrations decrease with increasing altitude above the tropical tropopause as a result of coagulation during the upward air transport produced by stratospheric circulations. During the extended periods of time that volcanic eruptions do not strongly influence stratospheric particle number concentrations, particles formed in the upper tropical troposphere provide nuclei upon which oxidized sulfur gases condense in the stratosphere. This particle source, coupled with aerosol microphysical properties and atmospheric transport, governs the number concentration of particles in the lower tropical and mid-latitude stratosphere.

The stratospheric aerosol layer, or Junge layer, is a fine mist of highly concentrated liquid sulfuric acid (H_2SO_4) particles that envelops the Earth at altitudes from a few kilometers above the tropopause (~9 to 17 km) to ~28 km. The particles are typically 0.1 to 0.3 μm in diameter and are present at number mixing ratios (NMR, number of particles per milligram of air) of ~60 mg^{-1} (*1–3*). These stratospheric H_2SO_4-H_2O particles provide sites for heterogeneous reactions that repartition nitrogen species, ultimately leading to reduced ozone concentrations (*4, 5*). In the polar regions, reactions on these particles may also activate chlorine, which catalytically destroys ozone (*6*). In both of these cases, the surface area provided by the particles for the heterogeneous reactions is an important parameter in the chemical process. In the polar vortices, H_2SO_4-H_2O particles are the nuclei on which polar stratospheric clouds (PSCs) form (*7*). Changes in the concentration of PSC nuclei may change the concentration of PSC particles, the surface area available for chlorine activation, and the process of particle sedimentation that leads to denitrification and polar ozone depletion (*8*).

The surface area available for heterogeneous reactions in the stratosphere depends largely on the number of particles upon which the total particle mass is distributed. Most of the mass of the stratospheric aerosol layer originates from reduced sulfur gases (OCS, CS_2, and SO_2) transported from the troposphere (*2*). These gases oxidize in the stratosphere to H_2SO_4, which then condenses onto preexisting particles (nuclei). In volcanically quiescent periods, OCS is believed to be the dominant source of stratospheric H_2SO_4 mass (*9*). The sources of the nuclei on which the H_2SO_4 condenses are poorly known. Many particles form in the stratosphere from homogeneous nucleation of H_2SO_4-H_2O after major volcanic injections of SO_2 (*10, 11*). However, within ~6 months after such eruptions, stratospheric NMRs decay to near prevolcanic values (*12*). When volcanic effects are small, the stratosphere's degree of supersaturation with H_2SO_4 vapor is insufficient for particle formation (*3, 10, 13*), with some minor exceptions (*14*). These findings im-

C. A. Brock, J. C. Wilson, H. H. Jonsson, Department of Engineering, University of Denver, Denver, CO 80208, USA.
P. Hamill, Department of Physics, California State University, San Jose, CA 95192, USA.
K. R. Chan, Ames Research Center, National Aeronautics and Space Administration, Moffett Field, CA 94035, USA.

*To whom correspondence should be addressed.